EXCELLENT PUBLISHERS

International Journal of Current Research and Academic Review

ISSN: 2347-3215 Volume 3 Number 7 (July-2015) pp. 31-45

www.ijcrar.com

Molecular structure, NMR, UV-Visible, vibrational spectroscopic and HOMO, LUMO analysis of phthalide using DFT calculations

V. Krishnakumar[1], M.Kumar[2]* and N.Jayamani[3]

[1]Department of Physics, Periyar University, Salem-636011, India
[2]Department of Physics, Government Arts College (Autonomous), Salem-636007, India
[3]Department of Physics, Vivekanandha College of Arts & Science (W), Namakkal-637205, India
Corresponding author

KEYWORDS

Phthalide,
Density functional theory,
FTIR,
FT-Raman,
Vibrational spectra,
1H and 13C NMR spectra,
HOMO and LUMO,
NBO

A B S T R A C T

Vibrational spectral analysis was carried out for phthalide by using the FTIR and FT-Raman spectroscopy in the range of 4000 cm^{-1}-400 cm^{-1} and 4000 cm^{-1}-50 cm^{-1} respectively. The theoretical computational density functional theory (DFT/B3LYP) was performed at 6-31G** levels to derive equilibrium geometry, vibrational wavenumbers, infrared intensities and Raman scattering activities. The complete vibrational assignment was performed on the basis of the potential energy distribution (PED), calculated with scaled quantum mechanics (SQM) method. Quantum chemical parameters such as the highest occupied molecular orbital energy (E_{HOMO}), the lowest unoccupied molecular orbital energy (E_{LUMO}), energy gap (ΔE), chemical potential (P_i), global hardness (η), and the softness (σ), were calculated. The theoretical electronic absorption spectra have been calculated by using CIS methods. ^{1}H and ^{13}C nuclear magnetic resonance (NMR) chemical shifts of the molecule were calculated by using gauge invariant atomic orbital (GIAO) method. The total atomic charges, natural charges and thermodynamic parameters were also calculated.

Introduction

In the past two decades, quantum chemical computational methods have been proven to be an essential tool for interpreting and predicting vibrational spectra (Hess *et al.*, 1986; Pulay *et al.*, 1993). A significant advancement in this area was made by combining semi-empirical quantum mechanical method; ab initio quantum mechanical method and density functional theory (DFT), each method having its own advantages (Blom and Altona, 1976; Ziegler, 1991; Shin *et al.*, 1998; Hehre *et al.*, 1986).

In the SQM approach, the systematic errors of the computed harmonic force field are corrected by a few scale factors which are found to be well transferable between chemically related molecules (Pulay *et al.*, 1993; Pulay *et al.*, 1979).

Phthalide is a lactone that serves as the core chemical structure for a variety of more complex chemical compounds including dyes, fungicides and natural oils (Kus, Nermin Simsek, 2008). Phthalide derivatives are used to manufacture the sensitizer or reverser of the antineoplastic agent. It enhances the sensitivity of drug-resistance, tumor cells against chemotherapy. It also used for the treatment and prevention Diabetes mellitus.

In this study, we recorded FT-IR, FT-Raman spectra and calculated the vibrational frequencies of phthalide in the ground state to distinguish fundamentals from experimental vibrational frequencies and geometric parameters using DFT/B3LYP (Becke3-Lee-yang-Parr) method. In addition, the gauge-invariant atomic orbital (GIAO) ^{13}C and ^{1}H chemical shifts calculations of the title compounds were calculated by using B3LYP/6-31G** basis set (Mehmet Karabaccak *et al.,* 2008). The calculated quantum chemical parameters are E_{HOMO}, E_{LUMO}, ΔE and those parameters that give valuable information about the reactive behavior such as chemical potential (P_i), global hardness (η), and the softness (σ) (Masoud *et al.,* 2010). A detailed quantum chemical study will aid in making definite assignments to fundamental normal modes of phthalide in clarify the experimental data for the important molecule.

Experimental

The compound phthalide in the solid form was purchased from sigma-Aldrich company (USA) with a stated purity of 99% and it was used as such without further purification. Fourier transform infrared (FTIR) were measured in the region of 4000-400 cm^{-1}. The FT-Raman spectrum of phthalide was recorded on a BRUKER IFS-66V model interferometer equipped with an FRA-106 and FT-Raman accessory. The spectra were recorded in the 4000-50cm^{-1} stokes region using 1064-nm line of a Nd: YAG laser for excitation operating at 200-mW power. The reported wavenumbers are believed to be accurate within ±1cm^{-1}.

The ^{1}H and ^{13}C NMR spectra were taken in $CDCl_3$ solution and all signals were referenced to TMS on a BRUKER FT-NMR spectrometer. All NMR spectra were measured at room temperature.

Calculations

All the calculations were performed by using GAUSSIAN 03W program (Frish *et al.,* 2003) package on the personal computer. The Becke's three-parameter hybrid density functional, B3LYP was used to calculate both harmonic and an harmonic vibrational wavenumbers with 6-31G** basis set. It is well known in the quantum chemical literature that the B3LYP functionals yields a good description of harmonic vibrational wave numbers for small and medium sized molecules. The optimized structural parameters were used in the vibrational frequency calculations at the DFT levels to characterize all stationary points as minima. The Cartesian representation of the theoretical force constants have been computed at the fully optimized geometry by assuming C_s point group symmetry for phthalide. The theoretical DFT force field were transformed from Cartesian into the local coordinates and then scaled empirically according to the SQM procedure (Pulay *et al.,* 1983).

$$F_{ij}^{Scaled} = (C_i C_j)^{\frac{1}{2}} F_{ij}^{B3LYP} .$$

Where C_i is the scale factor of coordinate i, F_{ij}^{B3LYP} is the B3LYP/6-31G** force constant in local coordinate and F_{ij}^{Scaled} is the scaled force constant.

The prediction of Raman intensities was carried out by following the procedure outlined below. The Raman activities (S_i) calculated by the GAUSSIAN 03W program and adjusted during the scaling procedure with the MOLVIB program were converted to relative Raman intensities (I_i) using the following relationship derived from the basic theory of Raman scattering (Polavarapu, 1990; Keresztury *et al.,* 1993; Keresztury, 2002).

$$I_i = \frac{f(\upsilon_o - \upsilon_i)^4 S_i}{\upsilon_i \left[1 - \exp\left(\frac{-hc\,\upsilon_i}{KT}\right)\right]}$$

Where υ_0 is the exciting frequency (in cm^{-1} units), υ_i the vibrational wave number of the *i*th normal mode, h, c and k are the fundamental constants and f is the suitably chosen common normalization factor for all the peak intensities.

The calculated quantum chemical parameters such as the highest occupied molecular orbital energy (E_{HOMO}), the lowest unoccupied molecular orbital energy (E_{LUMO}), energy gap (ΔE), chemical potential (P_i), global hardness (η) and the softness (σ) were calculated. The concepts of these parameters are related to each other (Parr *et al.*, 1978; Parr and Pearson, 1983; Pearson, 1988; Geerlings *et al.*, 2003). Where,

$P_i = -\chi$,
$P_i = (E_{HOMO} + E_{LUMO}) / 2$ and
$\eta = (E_{LUMO} - E_{HOMO}) / 2$.

The inverse value of the global hardness is designated as the softness σ, as follows:

$\sigma = 1/\eta$.

For NMR calculations, the title molecules are firstly optimized and after optimization, ^1H and ^{13}C NMR chemical shifts (H and C) were calculated using the GIAO method in $CDCl_3$ at B3LYP method with 6-31G** basis set (Ditchfield, 1972; Wolinski *et al.*, 1990). Absolute isotropic magnetic shielding was transformed into chemical shifts by referencing to the shielding of a standard compound (TMS) computed at the same level. It has been shown that B3LYP applications were successful in shielding calculations on carbon atoms (Wolinski *et al.*, 1990).

Results and Discussion

Molecular geometry

The molecular structure of phthalide with C_S symmetry is shown in figure 1. The global minimum energies obtained by the DFT structure optimization for phthalide are calculated as - 458.93170 hartrees. The bond length, bond angle and dihedral angle determined at the DFT level of theory for the phthalide compound are listed in table 1.

Assignment of Fundamentals

The vibrational bands observed in the IR region are very sharp, broad and less intense. The title compounds belong to C_s point group. The 16 atoms composing for phthalide structure has 42 fundamental modes of vibration. For molecule of C_s symmetry, group theory analysis indicates that the 42 fundamental vibrations are distributed among the symmetry species as,

Γ_{vib} =29A'(in–plane) +13A"(out–of–plane)

for phthalide. From the structural point of view of the molecule have 29 stretching vibrations, 13 bending vibrations. All the vibrations were found to be active both in Raman scattering and infrared absorption. The full set of 62 standard internal coordinates containing 20 redundancies are defined as given in table 2. From these a non-redundant set of local symmetry coordinates were constructed by suitable linear combination of internal coordinates are summarized in table 3.

The observed and calculated wave numbers, calculated IR and Raman intensities and normal mode descriptions (characterized by potential energy distribution (PED)) for the fundamental vibrations of phthalide depicted in table 4. For visual comparison, the observed and simulated FTIR and FT-Raman spectra of the compound are presented in figure 2 and figure 3 which help to understand the observed spectral features. The root mean square (rms) error of the observed and calculated wavenumbers (unscaled/ B3LYP/6-31G**) of phthalide was found to be 98.6 cm^{-1}. This is understandable since the mechanical force fields usually differ appreciably from the observed ones. This is partly due to the neglect of anharmonicity and partly due to approximate nature of the quantum mechanical methods. However for reliable information on the vibrational properties, the use of selective

scaling is necessary. The calculated wave numbers are scaled using the set of transferable scale factors recommended by Rauhut and Pulay (Rauhut and Pulay, 1995). The SQM treatment has resulted in an RMS deviation of 8.58 cm^{-1} for phthalide. The RMS values of wavenumbers were obtained in this study using the following expression,

$$RMS=\sqrt{\frac{1}{(n-1)}\sum_{i}^{n}\left(\upsilon_i^{calc}-\upsilon_i^{exp}\right)^2}$$

Table.1 Optimized geometrical parameters of phthalide obtained by B3LYP/6-31 G** density functional calculations

Bond length	Value(Å)	Bond angle	Value(°)
C1-C2	**1.3979**	**C1-C2-C3**	**121.3809**
C2-C3	**1.4032**	**C2-C3-C4**	**120.5211**
C3-C4	**1.3940**	**C3-C4-C5**	**117.5994**
C4-C5	**1.3931**	**C4-C5-C6**	**129.1709**
C5-C6	**1.4811**	**C5-C6-O7**	**107.3650**
C6-C7	**1.3790**	**C6-O7-C8**	**117.0984**
O7-C8	**1.4387**	**O7-C8-C9**	**105.1360**
C8-C9	**1.5067**	**C9-C1-H10**	**121.6445**
C1-H10	**1.0862**	**C1-C2-H11**	**119.3418**
C2-H11	**1.0860**	**C2-C3-H12**	**119.4833**
C3-H12	**1.0855**	**C3-C4-H13**	**122.0293**
C4-H13	**1.0852**	**C5-C6-O14**	**130.0371**
C6-O14	1.2046	O7-C8-H15	108.5311
C8-H15	1.0962	O7-C8-H16	108.5311
C8-H16	1.0962		

For numbering of atoms refer figure 1.

Table.2 Definition of internal coordinates of Phthalide

No.(i)	Symbol	Type	Definition
Stretching			
1-8	r_i	C-C	C1-C2,C2-C3,C3-C4,C4-C5,C5-C6,C8-C9, C9-C5, C9-C1
9-10	r_i	C-O	C6-O7, C8-O7.
11	r_i	C=O	C6-O14
12-17	r_i	C-H	C1-H10, C2-H11, C3-H12, C4-H13, C8-H15, C8-H16.
Bending			
18-23	β_i	bRing1	C1-C2-C3, C2-C3-C4, C3-C4-C5, C4-C5-C9, C5-C9-C1, C9-C1-C2
24-28	β_i	bRing2	C8-C9-C5, C9-C5-C6, C5-C6-07, C6-O7-C8, O7-C8-C9
29-30	β_i	bCO	C5-C6-O14, O7-C6-O14
31-42	β_i	bCH	C9-C1-H10, C2-C1-H10, C1-C2-H11, C3-C2-H1`1, C2-C3-H12, C4-C3-H12, C3-C4-H13, C5-C4-H13, O7-C8-H15, C9-C8-H15, O7-C8-H16, C9-C8-H16
Out-of-plane bending			
43-48	τ_i	trRng1	C1-c2-c3-c4, c2-c3-c4-c5, c3-c4-c5-c9, c4-c5-c9-c1, c5-c9-c1-c2, c9-c1-c2-c3

49-53	τ_i	tRing2	C8-c9-c5-c6, c9-c5-c6-o7, c5-c6-o7-c8, c6-o7-c8-c9, o7-c8-c9-c5
54-59	ω_i	gCH	C9-C2-C1-H10, C9-C3-C2-H11, C2-C4-C3-H12, C3-C5-C4-H13, O7-C9-C8-H15, MO7-C9-C8-H16
60	ω_i	gCO	C5-O7-C6-O14
61-62	ω_i	tButterfly	C1-C9-C5-C6, C8-C9-C5-C4

For numbering of atoms refer figure 1.

Table.3 Definition of natural internal coordinates of Phthalide

No. (i)	Symbol[a]	Definition[b]
1-8	C-C Stretch	r_1,r_2,r_3,r_4, r_5, r_6,r_7,r_8.
9-10	C-O Stretch	r_9,r_{10}
11	C=O Stretch	r_{11}
12-17	C-H Stretch	r_{12}, r_{13}, r_{14}, r_{15}, r_{16}, r_{17}
18	Rtrigd	$(\beta_{18}-\beta_{19}+\beta_{20}-\beta_{21}+\beta_{22}-\beta_{23})/\sqrt{6}$
19	Rsymd	$(-\beta_{18}-\beta_{19}+\beta_{20}-\beta_{21}-\beta_{22}+2\beta_{23})/\sqrt{12}$
20	Rasymd	$(\beta_{19}-\beta_{20}+\beta_{22}-\beta_{23})/2$
21	Rbend1	$(\beta_{24}+a(\beta_{25}+\beta_{28})+b(\beta_{26}+\beta_{27})$
22	Rbend2	$(a-b)(\beta_{24}-\beta_{28})+(1-a)(\beta_{26}-\beta_{27})$
23	bCO	$(\beta_{29}-\beta_{30})/\sqrt{2}$
24-29	bC-H	$(\beta_{31}-\beta_{32})/\sqrt{2}$,$(\beta_{33}-\beta_{34})/\sqrt{2}$,$(\beta_{35}-\beta_{36})/\sqrt{2}$,$(\beta_{37}-\beta_{38})/\sqrt{2}$, $(\beta_{39}-\beta_{40})/\sqrt{2}$, $(\beta_{41}-\beta_{42})/\sqrt{2}$
30	ttrigd	$(\tau_{43}-\tau_{44}+\tau_{45}-\tau_{46}+\tau_{47}-\tau_{48})/\sqrt{6}$
31	tsymd	$(\tau_{43}-\tau_{44}+\tau_{46}+\tau_{47})/2$
32	tasymd	$(-\tau_{42}+2\tau_{43}-\tau_{44}-\tau_{45}+\tau_{46}-\tau_{47})/\sqrt{12}$
33	tRtorsion1	$b(\tau_{49}+\tau_{53})+a(\tau_{50}+\tau_{51})+\tau_{52}$
34	tRtorsion1	$a-b(\tau_{53}-\tau_{49})+(1-a)(\tau_{51}-\tau_{50})$
34	ωC-O	ω_{54}
36-41	ωC-H	ω_{55}, ω_{56}, ω_{57}, ω_{58}, ω_{59}, ω_{60}
42	t Butterfly	$(\tau_{61}-\tau_{62})/2$

[a]These symbols are used for description of the normal modes by PED in Table.
[b]The internal coordinates used here are defined in Table.

Fig.1 Optimized structure of Phthalide

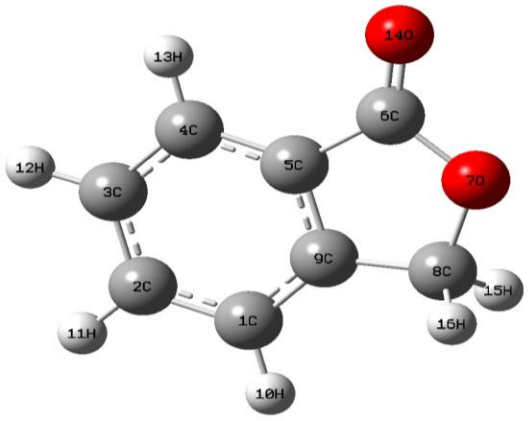

Table.4 Detailed assignment of fundamental vibrations of Phthalide by normal mode analysis based on SQM force field calculations

Sl. No	Symmetry species C_s	Observed wave numbers cm^{-1}		Calculated wave numbers B3LYP/6-31G** force field cm^{-1}		IR Intensity	Raman Activity	Characterization of normal modes with PED (%)
				Unscaled	scaled			
		FT IR	Raman					
1.	A'	-	3099	3217	3088	2.5273	1.7983	υOH(87)
2.	A'	-	3067	3206	3046	0.4413	4.0414	υCH(98)
3.	A'	-	3064	3185	3026	3.4897	0.6389	υCH(88)
4.	A'	-	2982	3176	2953	4.3884	1.5381	υCH(91)
5.	A'	-	2950	3086	2931	0.4647	0.0233	υCH(100)
6.	A'	-	2945	3048	2896	4.7697	0.5739	υCH(100)
7.	A'	-	1770	1874	1780	0.0156	8.0450	υC=O(89)
8.	A'	1615	-	1669	1586	1.9534	4.5484	υCC(59)
9.	A'	1603	-	1654	1571	2.6084	0.8058	υCC(61)
10.	A'	1468	-	1518	1442	7.5005	0.7275	bCCH(59)
11.	A'	-	1447	1509	1433	1.1555	0.3700	bCCH(47), υCC(12)
12.	A'	1440	-	1506	1431	46.0880	1.5200	υCC(26), bCCH(17), bring(15)
13.	A'	1369	-	1401	1331	0.8703	19.7209	υCC (28), bCCH(24)
14.	A'	1341	-	1360	1292	8.1013	0.4017	υCC (39), bCCH(18)
15.	A'	1289	-	1312	1246	0.0846	6.6892	bCCH(68)
16.	A'	-	1226	1240	1178	0.0147	4.3463	υCC(42), bCCH(10)
17.	A'	1200	1200	1212	1151	0.5294	1.0549	bCCH(23), bCCO(14), bring(12), υCC(11)
18.	A'	1188	-	1205	1145	0.0000	0.0574	bOCH(93)
19.	A'	1167		1184	1125	0.0157	0.4012	bCCH(48)
20.	A'	1111	-	1122	1066	35.9010	11.0051	υCC (31), bring(17), bCCH (14)

21.	A'	1046	-	1063	1010	20.0728	5.1015	υCO(55), bring(10)
22.	A'	-	1022	1050	998	140.3704	3.7302	υCO(16), υCC(14), bCO(10)
23.	A'	1020	-	1037	985	15.8730	1.9306	υCC(52), bCO(20), bring (14)
24.	A″	1010	-	1030	979	4.0324	6.5312	ωCH(43)
25.	A″	-	1000	1003	953	0.3653	8.6094	ωCH(82)
26.	A″	952	-	964	916	14.3653	4.7575	ωCH(84)
27.	A″	-	863	891	846	21.6595	23.5011	ωCH(77)
28.	A″	800	-	855	838	36.3621	7.3165	ωCH (57), tRing(18)
29.	A″	-	767	797	757	25.1765	16.5270	ωCH(49), tRing (28)
30.	A'	764	-	776	737	29.1846	11.3434	bring(55), υCC (11)
31.	A″	716	-	742	705	2.3470	7.7547	tRing (41), ωCH(39)
32.	A'	701	-	707	672	14.6882	12.0610	bring (63)
33.	A″	681	-	689	655	1.7059	11.6769	tRing (73)
34.	A'	592	-	595	565	2.7454	23.5800	bring (48), υCC(11)
35.	A'	565	-	571	542	15.8637	17.7653	bring (53)
36.	A'	481	-	495	470	435.8335	55.8139	bring(31), υCC(30)
37.	A″	474	-	481	457	29.1971	213.7345	tRing (70)
38.	A″	-	415	423	402	17.2803	118.6439	ttRing (78)
39.	A'	-	260	277	263	1.0976	54.6599	bCO(77)
40.	A″	-	203	236	224	10.0702	101.9479	tRing(54), ωCH(33)
41.	A″	-	170	184	175	14.0699	113.3197	tButterfly(68)
42.	A″	-	-	141	1332	8.7345	186.5286	ωCO(62), tRing(14)

Abbreviations; R, ring; b, bending; deform, deformation; sym, symmetric; asy, asymmetric; ω, wagging; t, torsion; trig, trigonal; υ, stretching; ips, in – plane stretching; ipb, in –plane bending; ops, out - of - plane stretching; opb, out - of - plane bending; sb, symmetric bending; ipr, in - plane rocking; opr, out – of – plane rocking. Only contributions larger than 10 % are given.

Table.5 Atomic charges for optimized geometry of Phthalide obtained by B3LYP/6-31 G** density functional calculations

Atoms	Mulliken
C1	**-0.1301**
C2	-0.0791
C3	-0.0907
C4	**-0.1079**
C5	**0.0275**
C6	0.5736
O7	-0.4841
C8	0.0244
C9	0.0383
H10	**0.0960**
H11	**0.0991**
H12	**0.0997**
H13	**0.1201**
O14	**-0.4599**
H15	**0.1364**
H16	**0.1364**

For numbering of atoms refer figure 1.

Table.6 Theoretical electronic absorption spectra values

S. No	Calculated/λ_{cal} (nm) CIS		
	Excitation Energies (ev)	**Oscillator strength**	**Wavelength (nm)**
1.	5.7623	0.0002	215.16
2.	5.8202	0.0934	213.02
3.	6.0460	0.0445	205.07

Table.7 Calculated quantum chemical parameters of the phthalide derivatives

Parameters	**B3LYP/6-31G**
E_{HOMO}	-0.26684
E_{LUMO}	-0.04983
ΔE	-0.21701
X	0.158335
η	-0.108505
σ	-9.21616

Table.8 Calculated ^{13}C NMR Chemical shifts (ppm) of Phthalide

Carbon	Exp	B3LYP/6-31G**
C1	171.06	179.85
C2	125.45	151.81
C3	146.72	174.37
C4	128.99	166.30
C5	134.07	172.53
C6	125.64	155.92
C8	69.76	59.45
C8	122.35	97.85

For numbering of atoms refer figure 1

Table.9 Experimental and calculated ^{1}H NMR Chemical shifts (ppm) of Phthalide

Proton	Exp	B3LYP/6-31G**
H10	7.50	4.99
H11	5.33	4.60
H12	5.33	4.85
H13	7.60	5.49
H15	7.91	7.09
H16	7.68	7.09

For numbering of atoms refer figure 1

Fig.2 Comparison of observed and calculated FTIR spectra of Phthalide calculated (b) observed
Wavenumber (cm^{-1})

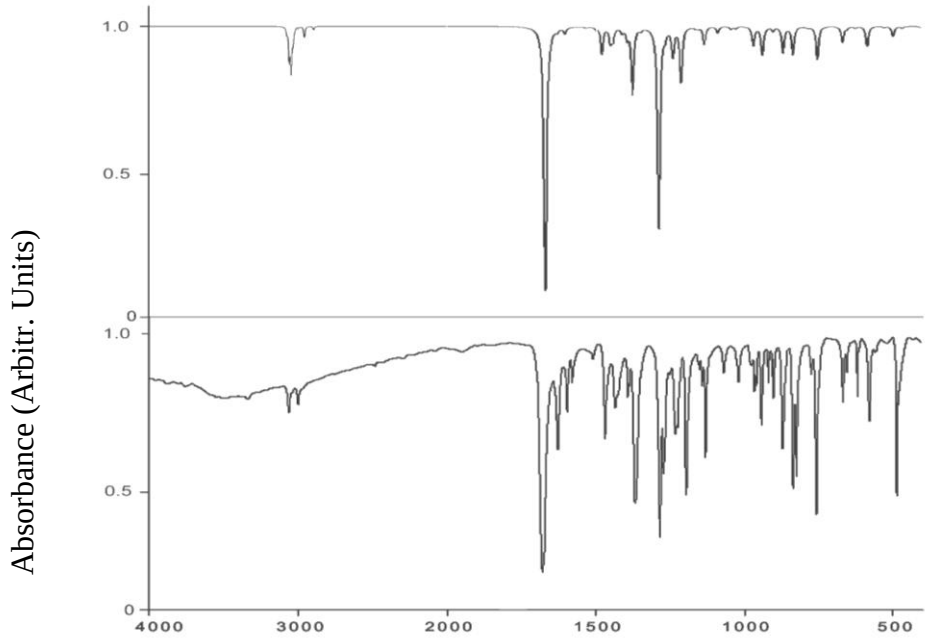

(a)

Fig.3 Comparison of observed and calculated FT-Raman spectra of phthalide
(a) calculated **(b)**observed

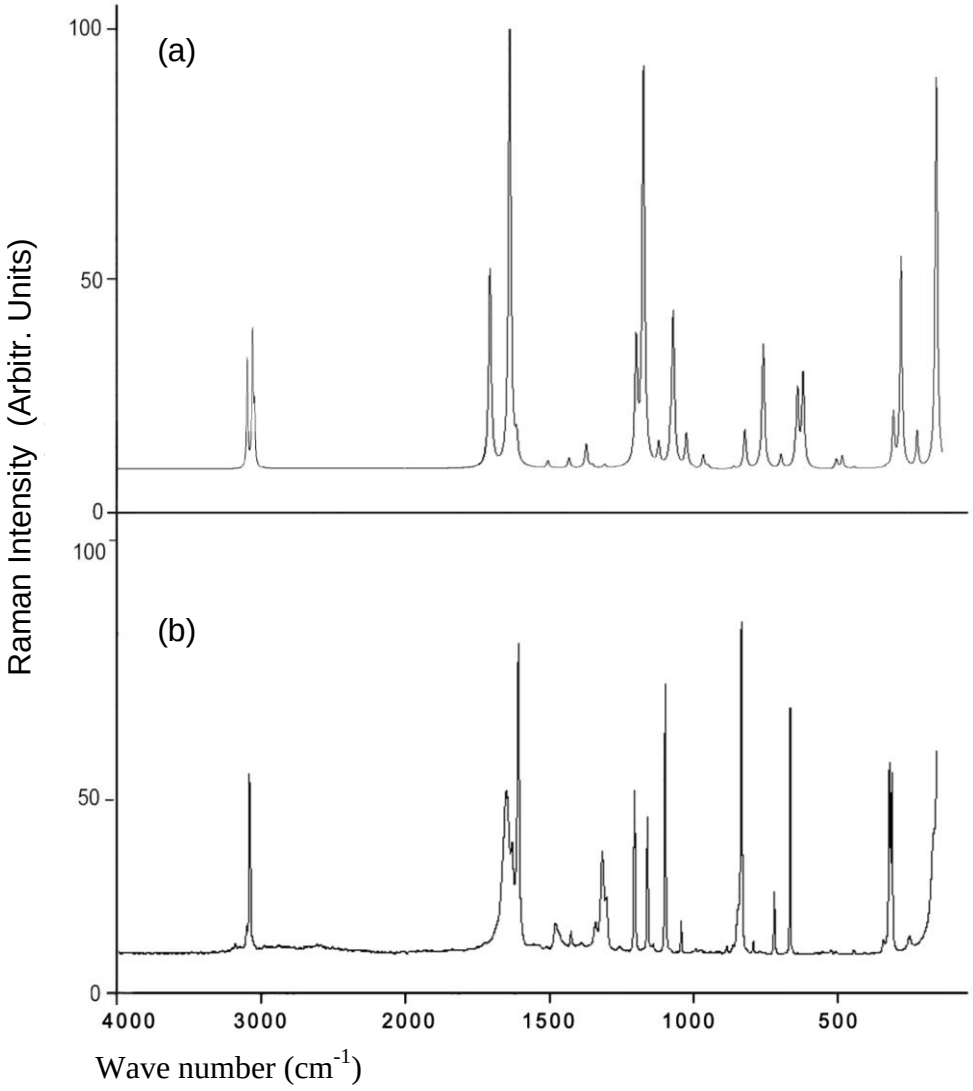

Fig.4 Surfaces of HOMO, LUMO for the Phthalide

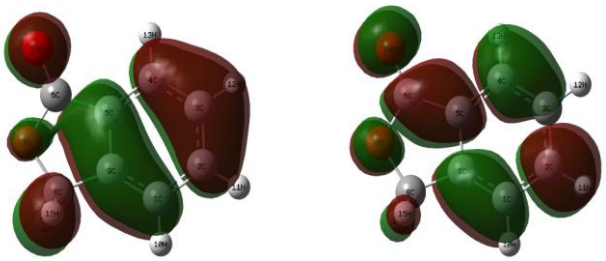

Fig.5 Plot of the calculated vs. the experimental ^{13}C NMR, ^{1}H NMR chemical shifts (ppm) for Phthalide

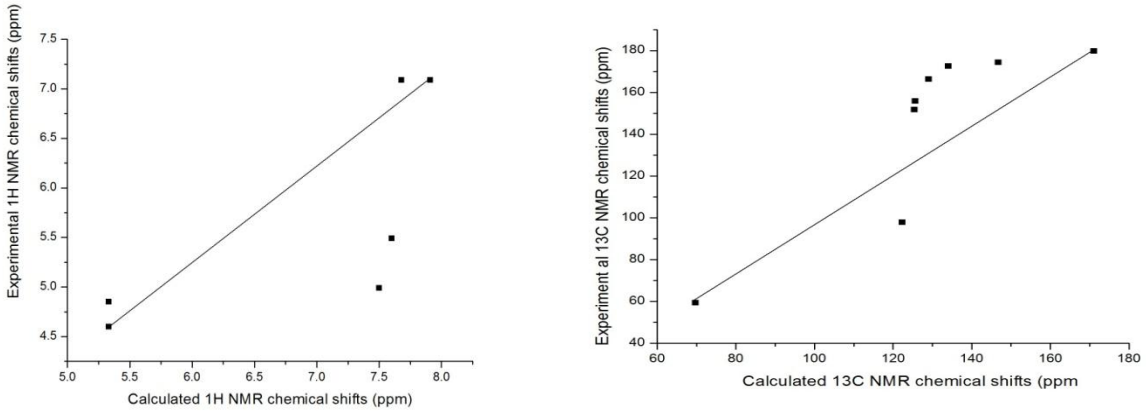

Fig.6 Electrostatic potential (ESP for phthalide)

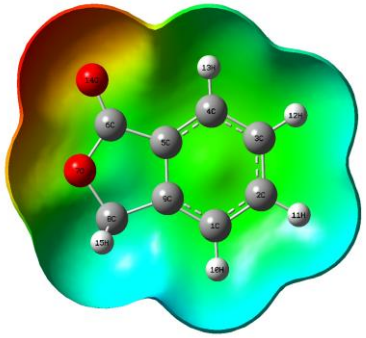

CH Vibrations

The heterocyclic structure shows the presence of C-H stretching vibrations around 3000 cm^{-1} (Collier and Klotts, 1995; Mohan *et al.*, 1991). In phthalide these bands are observed at 3099, 3067, 3064, 2982, 2950 and 2945 cm^{-1} in FT-Raman spectrum. The C-H in-plane deformations are obtained at 1468, 1447, 1289, 1200 and 1188 cm^{-1} in FTIR and FT-Raman spectrum. The C-H out-of-plane bending modes are observed at 1010, 1000, 952, 863, 800 and 767 cm^{-1} in FTIR and FT-Raman spectrum.

Ring Vibrations

Ring stretching modes (C=C, C-O) appears in narrow spectral region 1640-1400 cm^{-1} and 1150-925 cm^{-1} (George Socrates, 2001). In the present work, the C=C stretching vibrations are attributed at 1615, 1603, 1440, 1369, 1341, 1226, 1111 and 1020 cm^{-1} in FT-IR and FT-Raman spectrum. The C-O stretching modes are observed at 1046 and 1022 cm^{-1} in FT-IR and FT-Raman spectrum. The in-plane and out-of-plane deformations are assigned within the characteristic region and reported in table 4.

C=O vibrations

The title molecule is acquiring a highly polar bond containing carbon and oxygen which is formed by p_{π}-p_{π} between carbon and oxygen. Because of the different eletronegativities of carbon and oxygen atoms, the bonding electrons

are not equally distributed between the two atoms. The following two resonance forms contribute to the bonding of the carbonyl group.

$> C=O \leftrightarrow > C^{+} - O^{-}$

The lone pair of electrons on oxygen also determines the nature of carbonyl group. The carbonyl stretching mode is identified at 1770 cm^{-1} in FT-Raman spectrum (George Socrates, 2001; Krishna Kumar and Balachandran, 2005). The in-plane and out-of-plane deformation for the carbonyl group is given in table 4.

Electronic properties

Atomic charges on the various atoms of phthalide obtained by Mulliken population analysis (Forgarasi and Pulay, 1985) are given in table 5.

The theoretical electronic absorption spectra for the title compounds were calculated at B3LYP/6–31G** using CIS method and absorption maxima are listed in table 6. The theoretical electronic excitation energies, oscillator strengths, absolute energies, and nature of the singlet-singlet excitations were also calculated for the water solvents. Calculations of the molecular orbital geometry show that the visible absorption maxima of the molecule correspond to the electron transition between frontier orbitals such as translation from HOMO to LUMO. We performed an analysis of all the molecular orbitals involved, taking into consideration that orbital 40 is the HOMO and orbital 41 is the LUMO for phthalide.

Highest occupied molecular orbital and lowest unoccupied molecular orbital are very important parameters for quantum chemistry. This is also used by the frontier electron density for predicting the most reactive position in π-electron systems and also explains several types of reaction in conjugated system (Fukuli *et al.,* 1952). The conjugated molecules are characterized by a small highest occupied molecular orbital-lowest unoccupied molecular orbital (HOMO-LUMO) separation, which is the result of a significant degree of intermolecular charge transfer from the end-capping electron-donar groups to the efficient electron-acceptor groups through π conjugated path (Choi and Kertesz, 1997). Both the highest occupied molecular orbital and lowest unoccupied molecular orbital are the main orbitals take part in chemical stability (Gunasekaran *et al.,* 2008). Energy difference between HOMO and LUMO orbital is called as energy gap that is an important stability for structures which are given in table 7.

Many organic molecules that contain conjugated π electrons are characterized as hyper-polarisabilities and are analyzed by means of vibrational spectroscopy. The analysis of the wave function indicates that the electron absorption corresponds to the transition from the ground state to the first excited state and is mainly described by the one-electron excitation from the HOMO to the LUMO. The HOMO, of π nature (i.e., aromatic ring) is delocalized over the whole C-C bond. By contrast, the LUMO is located over the aromatic ring. Consequently, the HOMO-LUMO transition implies an electron density transfer to hydroxyl and ester group from the aromatic ring. The atomic orbital compositions of the frontier molecular orbitals are sketched in figure 4.

NMR spectra

DFT methods treat the electronic energy as a function of the electron density of all electrons simultaneously and thus include electron correlation effect (Avci *et al.,* 2009). In this study, molecular structure of phthalide was optimized by using B3LYP method in conjunction with 6-31G**. ^{13}C and ^{1}H chemical shift calculations of the title compound has been made by using GIAO method and same basis set. The isotropic shielding values were used to calculate the isotropic chemical shifts δ with respect to tetramethylsilane (TMS). The isotropic chemical shifts are frequently used as an aid in identification of reactive ionic species. The B3LYP method allows calculating the shielding constants with the proper accuracy, and the GIAO method is one of the most common approaches for calculating nuclear magnetic shielding tensors.

Theoretical and experimental chemical shifts of phthalide in ^{1}H and ^{13}C NMR spectra are gathered in tables 8 and 9. The range of the $^{13}CNMR$ chemical shifts for typical organic molecules usually is >100 ppm (Kalinowski *et al.*, 1988; Pihlaja and Kleinpeter, 1994) and the accuracy ensures reliable interpretation of spectroscopic parameters. In the present study, the $^{13}CNMR$ chemical shifts in the ring are >100 ppm, as they would be expected.

The linear correlations between calculated and experimental data of $^{13}CNMR$ and $^{1}HNMR$ spectra are determined as 0.86659 and 0.72460 for phthalide. There is an excellent linear relationship between experimental and computed results which are shown in figure 5.

Electrostatic potential

Electrostatic potential maps also known as electrostatic potential energy maps or molecular electrical potential surfaces, illustrate the charge distributions of molecules in three dimensionally. These maps allow us to visualize variably charged regions of a molecule. Knowledge of the charge distributions can be used to determine how molecules interact with one another. An advanced computer program calculates the electrostatic potential energy at a set of distance from the nuclei of the molecule. Electrostatic potential energy is fundamentally a measure of the strength of the nearby charges, nuclei and electrons at a particular position.

In the present study, the electrostatic potential (ESP) of phthalide is illustrated in figure 6. To accurately analyze the charge distribution of a molecule, a very large quantity of electrostatic potential energy values must be calculated. The best way to convey this data is to visually represent it, as in an electrostatic potential map. A computer program then imposes the calculated data onto an electron density model of the molecule derived from the Schrödinger equation. To make the electrostatic potential energy data easy to interpret, a colour spectrum, with red as the lowest electrostatic potential energy value and blue as the highest, is employed to convey the varying intensities of the electrostatic potential energy values (Murray and Sen, 1996).

The electrostatic potential (ESP) is a physical property of a molecule related to how a molecule is first “seen” or “felt” by another approaching species. A portion of a molecule that has a negative electrostatic potential is susceptible to electrophilic attack-the more negative the better. The MESP simultaneously displays molecular shape, size and electrostatic potential values and has been plotted for the title molecule. MESP mapping is very useful in the investigation of the molecular structure with its physiochemical property relationships (Gadre and Shirsat, 2001). The different values of the electrostatic potential at the surface are represented by different colours; red represents regions of most negative electrostatic potential, blue represents regions of almost positive electrostatic potential and green represents region of zero potential. Potential decreases in the order red < orange < yellow <green < blue.

Conclusion

Attempts have been made in the present work for the molecular parameters and frequency assignments for phthalide from the FTIR and FT-Raman spectra. The equilibrium geometries, harmonic and anharmonic frequencies for the title compound were determined and analyzed at DFT level of theory utilizing B3LYP/6-31G** basis set. The assignments of most of the fundamentals of the title compound provided in this work are quite comparable. The excellent agreement of the calculated and observed vibrational spectra reveals the advantages of a smaller basis set for quantum chemical calculations. The absorption wavelength (λ), excitation energies and oscillator strengths (f) were calculated. HOMO and LUMO energy gap explains the eventual charge transfer interactions taking place within the molecule. The experimental and theoretical investigation of the title compound has been performed successfully by using ^{1}H and ^{13}C NMR. The various modes of vibrations were unambiguously assigned on the basis of the result of the PED output is obtained from normal coordinate analysis.

References

Avci, D., Atalay, Y., Sekerci, M., Dincer, M. 2009. Molecular structure and vibrational and chemical shift assignments of 3-(2-Hydroxyphenyl)-4-phenyl-1H-1,2,4-triazole-5-(4H)-thione by DFT and ab initio HF calculations, Spectrochim. Acta A 73: 212–217.

Blom, C.E., Altona, C. 1976. Application of self-consistent-field ab initio calculations to organic molecules. *Mol. Phys.,* 31: 1377–1391.

Choi, C.H., Kertesz, M. 1997. Conformational Information from vibrational spectra of styrene, trans-stilbene, and cis-Stilbene. *J. Phys. Chem.,* 101A: 3823–3831.

Collier, W.V., Klotts, T.D. 1995. Heteroatom derivatives of indene Part 3. Vibrational spectra of benzoxazole, benzofuran, and indole. *Spectrochim. Acta part A,* 51: 1291–1316.

Ditchfield, R. 1972. Molecular orbital theory of magnetic shielding and magnetic susceptibility. *J. Chem. Phys.,* 56: 5688–5691.

Forgarasi, G., Pulay, P. 1985. In: J.R. Durig (Ed.), Vibrational spectra and structure, Vol. 14. Elsevier, Amsterdam. Pp. 125–219.

Frish, M.J., *et al.* 2003. Gaussian 03, Revision B.4, Gaussian Inc., Pittsburgh, PA.

Fukuli, K., Yonezawa, T., Shingu, H. 1952. A molecular orbital theory of reactivity in aromatic hydrocarbons. *J. Chem. Phys.,* 20: 722–725.

Gadre, S.R., Shirsat, R.N. 2001. Electrostatics of atoms and molecules. Universities Press.

Geerlings, P., De Proft, F., Langenaeker, W. 2003. Conceptual density functional theory. *Chem. Rev*., 103: 1793–1874.

George Socrates, 2001. Infrared and Raman characteristic group frequencies – tables and charts, 3rd edn., John Wiley & sons, New York.

Gunasekaran, S., Balaji, R.A., Kumerasan, S., Anand, G., Srinivasan, S. 2008. Experimental and theoretical investigations of spectroscopic properties of N-acetyl-5-methoxytryptamine. *Can. J. Anal. Sci. Spectrosc.,* 53: 149–162.

Hehre, W.J., Random, L., Schleyer, P.V.R., Pople, J.A. 1986. Ab initio Molecular Orbital Theory, Wiley, New York.

Hess, B.A. Jr., Schaad, L.J., Carsky, P., Zahradnik, R., Ab initio calculations of vibrational spectra and their use in the identification of unusual molecules. *Chem. Rev.,* 86: 709–730.

Js Murray, K. Sen, 1996. Molecular electrostatic potentials, concepts and applications. Elsevier, Amsterdam.

Kalinowski, H.O., Berger, S., Braun, S. 1988. In: Carbon13 NMR Spectroscopy; John Wiley Sons: Chichester.

Keresztury, G. 2002. Raman spectroscopy: Theory in handbook of vibrational spectroscopy, Vol. 1. J.M. Chalmers, P.R. Griffiths (Eds), John Wiley & Sons, Ltd. Pp. 55–71.

Keresztury, G., Holly, S., Varga, J., Besenyei, G., Wang, A.Y., Durig, J.R. 1993. Vibrational spectra of monothiocarbamates-II. IR and Raman spectra, vibrational assignment, conformational analysis and ab initio calculations of S-methyl-N,N-dimethyl thiocarbamate. *Spectrochim. Acta Part A,* 49: 2007–2026.

Krishna Kumar, V., Balachandran, V. 2005. DFT studies, vibrational spectra and conformational stability of 4-hydroxy-3-methylacetophenone and 4-hydroxy-3-methoxyacetophenone. *Spectrochem. Acta part A,* 61: 2510–2525.

Kus, Nermin Simsek, 2008. Some oxidation reactions with molecular oxygen in subcritical water. *Asian J. Chem.,* 20: 1226–1230.

Masoud, M.S., Awad, M.K., Shaker, M.A., EI Tahaway, M.M.T. 2010. The role of structural chemistry in the inhibitive performance of some aminopyrimidines on the corrosion of steel. *Corros. Sci.,* 52: 2387–2396.

Mehmet Karabaccak, Ali Coruh, Mustafa Kurt, 2008. FT-IR, FT-Raman, NMR spectra, and molecular structure investigation of 2,3-dibromo-N-methylmaleimide: A combined experimental and theoretical study. *J. Mol. Struct.,* 892: 125–131.

Mohan, S., Sundaraganesan, N., Mink, J. 1991. FTIR and Raman studies on benzimidazole. *Spectrochim Acta part A*, 47A: 1111–1115.

Parr, R.G., Donnelly, D.A., Levy, M., Palke, W.E. 1978. Electronegativity: The density functional viewpoint. *J. Chem. Phys.*, 68: 3801–3807.

Parr, R.G., Pearson, R.G. 1983. Absolute hardness: companion parameter to absolute electronegativity. *J. Am. Chem. Soc*., 105: 7512–7516.

Pearson, R.G. 1988. Absolute electronegativity and hardness: application to inorganic chemistry. *Inorg. Chem.*, 27: 734–740.

Pihlaja, K., Kleinpeter, E. (Eds.). 1994. Carbon-13 NMR Chemical Shifts in Structural and Sterochemical Analysis, VCH Publishers, Deerfield Beach.

Polavarapu, P.L. 1990. Ab initio vibrational Raman and Raman optical activity spectra, *J. Phys. Chem.*, 94: 8106–8112.

Pulay, P., Fogarasi, G., Pongor, G., Boggs, J.E., Vargha, A. 1983. Combination of theoretical ab initio and experimental information to obtain reliable harmonic force constants. Scaled quantum mechanical (QM) force fields for glyoxal, acrolein, butadiene, formaldehyde, and ethylene. *J. Am. Chem. Soc.*, 105: 7037–7047.

Pulay, P., Forgarasi, G., Pong, F., Boggs, J.E. 1979. Systematic ab initio gradient calculation of molecular geometries, force constants, and dipole moment derivatives. *J. Am. Chem. Soc.*, 101: 2550–2560.

Pulay, P., Zhou, X., Forgarasi, G. 1993. In: NATO ASI Series, Vol. C40, R. Fausto (ed). Dordrecht, Kluwer. 99 Pp.

Rauhut, G., Pulay, P. 1995. Transferable scaling factors for density functional derived vibrational force fields. *J. Phys. Chem.*, 99: 3093–3100.

Shin, D.N., Hahn, J.W., Jung, K.H., Ha, T.K. 1998. Study of the Cis and Trans conformers of 2-halophenols using coherent anti-stokes Raman spectroscopic and quantum chemical method. *J. Raman Spectrosc.*, 29: 245–249.

Wolinski, K., Hinton, J.F., Pulay, P. 1990. Efficient implementation of the gauge-independent atomic orbital method for NMR chemical shift calculations. *J. Am. Chem. Soc.*, 112: 8251–8260.

Ziegler, T. 1991. Approximate density functional theory as a practical tool in molecular energetics and dynamics. *Chem. Rev.*, 91: 651–667.